BNL-105248-2014-TECH

Booster Technical Note No. 204;BNL-105248-2014-IR

TOPICS ON RF BEAM CONTROL OF A SYNCHROTRON

S. Y. Zhang

February 1992

Collider Accelerator Department

Brookhaven National Laboratory

U.S. Department of Energy

USDOE Office of Science (SC)

DISCLAIMER

TOPICS ON RF BEAM CONTROL OF A SYNCHROTRON

BOOSTER TECHNICAL NOTE
NO. 204

S. Y. ZHANG and W. T. WENG

February 4, 1992

ALTERNATING GRADIENT SYNCHROTRON DEPARTMENT
BROOKHAVEN NATIONAL LABORATORY
UPTON, NEW YORK 11973

TOPICS ON RF BEAM CONTROL OF A SYNCHROTRON *

S. Y. Zhang and W. T. Weng

AGS Department, Brookhaven National Laboratory,
Upton, New York 11973

ABSTRACT

In this paper, several typical situations of longitudinal motion in synchrotron design and operation are studied. The study is based on a unified beam dynamic model of synchrotron oscillation under phase and radial feedbacks. Cases studied include frequency error, lock-in range, bunch excursion, phase manipulation, injection and field errors.

TOPICS ON RF BEAM CONTROL OF A SYNCHROTRON *

S. Y. Zhang and W. T. Weng

AGS Department, Brookhaven National Laboratory,

Upton, New York 11973

I. Introduction

In a synchrotron, particles having energy deviation from the synchronous particle (s.p.) execute synchrotron oscillation around the s.p.[1]. The longitudinal synchrotron motion of the bunch as a whole in the absence of beam control can be regarded as a second order oscillatory system. With phase and radial controls, the beam can be manipulated by controlling the energy gain per turn in passing through the RF cavities, and thus the synchrotron motion can be modified to provide damping and to give rise to smaller radius and phase errors.

The problems and methods of RF beam control have been extensively discussed in past [2-8]. Our study here is based on a unified beam dynamic model of

* Work performed under the auspices of the U.S. Department of Energy

synchrotron oscillation under phase and radial feedback control [9]. Analysis on topics related to RF beam control of a synchrotron is carried out using this model and AGS Booster parameters. Cases studied include frequency error, lock-in range, bunch excursion, phase manipulation, injection and field errors.

II. Phase and Radial Feedbacks

1. Beam Dynamic Model

The simplified beam dynamic model for synchrotron oscillation can be shown in Fig.1, where s is the Laplace operator. Other variables are as follows.

B is the magnetic field.

ω_{rf} and ω_{id} are the cavity accelerating frequency and the ideal beam frequency, respectively.

$\Delta\phi$ and ΔR are the beam phase and radial deviations from the equilibrium state, respectively.

ΔE and $\Delta\omega_b$ are the beam energy and frequency deviations, respectively, and E is the total energy of the particle.

V is the RF voltage amplitude, which is independently preprogrammed.

ϕ_s is the stable phase, it is determined by the derivative of the magnetic field and the RF voltage V.

β is the ratio of the particle velocity v and the light velocity c.

R is the mean radius of the accelerator.

γ_t is the beam transition energy.

η is the frequency slip factor.

By inspecting the model in Fig.1, one obtains [9]

$$s\,\Delta\phi = -\frac{\omega_{id}\,\eta\gamma_t^2}{R}\,\Delta R + \delta\omega \tag{1a}$$

$$s\,\Delta R = -\frac{eV\cos\phi_s\,c}{2\pi\gamma_t^2\beta E}\,\Delta\phi \tag{1b}$$

To simplify the notation, we define

$$a = -\frac{\omega_{id}\,\eta\gamma_t^2}{R} \tag{2}$$

$$b = -\frac{eV\cos\phi_s\,c}{2\pi\gamma_t^2\beta E} \tag{3}$$

Thus the equation (1) can be written as

$$s\,\Delta\phi = a\,\Delta R + \delta\omega \tag{4a}$$

$$s\,\Delta R = b\,\Delta\phi \tag{4b}$$

where a and b are the machine parameters considered to be constant during the period of concern.

The simplified model can now be represented as in Fig.2. Note that a block T has been added for the oscillators and cavities, indicating that all regulations and controls will go through these elements. If the errors from them is neglected, T can be set to 1.

The transfer function from the input frequency perturbation $\delta\omega$ to the radial and phase deviations can therefore be obtained by eliminating mixed variables in equation (4), giving

$$\Delta R = T_1\,\delta\omega = \frac{b}{s^2 - ab}\,\delta\omega = \frac{b}{s^2 + \Omega_s^2}\,\delta\omega \tag{5}$$

$$\Delta\phi = T_2\,\delta\omega = \frac{s}{s^2 - ab}\,\delta\omega = \frac{s}{s^2 + \Omega_s^2}\,\delta\omega \tag{6}$$

where

$$\Omega_s = (-ab)^{1/2} = \left(-\frac{\omega_{id}\,eV\,\eta\cos\phi_s\,c}{2\pi R\,\beta E}\right)^{1/2} \tag{7}$$

is the synchrotron oscillation angular frequency.

2. Phase and Radial Feedbacks

The block diagram including phase and radial feedbacks can be represented by Fig.3. In the absence of G_2, G_1 alone represents the phase feedback, and the transfer functions from $\delta\omega$ to ΔR and $\Delta\phi$ with the phase feedback alone are as follows,

$$\Delta R = T_3\,\delta\omega = \frac{T_1}{1 + G_1 T_2}\,\delta\omega = \frac{b}{s^2 + k_1 s + \Omega_s^2}\,\delta\omega \tag{8}$$

$$\Delta\phi = T_4\,\delta\omega = \frac{T_2}{1 + G_1 T_2}\,\delta\omega = \frac{s}{s^2 + k_1 s + \Omega_s^2}\,\delta\omega \tag{9}$$

where we let $G_1 = k_1$, a simple amplifier.

When the radial feedback is added, the transfer functions become,

$$\Delta R = T_5\,\delta\omega = \frac{T_3}{1 + G_2 k_1 T_3}\delta\omega = \frac{b}{s^2 + k_1 s + \Omega^2}\,\delta\omega \tag{10}$$

$$\Delta\phi = T_6\,\delta\omega = \frac{T_4}{1 + G_2 k_1 T_3}\delta\omega = \frac{s}{s^2 + k_1 s + \Omega^2}\,\delta\omega \tag{11}$$

where $G_2 = k_2$, and

$$\Omega = (b k_1 k_2 + \Omega_s^2)^{1/2} \tag{12}$$

is the new coherent oscillation frequency under feedback control. For the second order system, the term Ω is called the natural frequency. With only the phase feedback, the natural frequency equals the synchrotron oscillation frequency given in equation (7), while for phase plus radial feedback, the natural frequency is higher than the synchrotron frequency, as shown in (12). The damping ratio is defined as

$$\varsigma = \frac{k_1}{2\Omega} \tag{13}$$

If $\varsigma = 1$, the system is critically damped. Thus, it is clear that a phase feedback can provide damping, while radial feedback can increase the natural frequency. It has been shown that the residual radius error for an unit step accelerating frequency error is [9]

$$\lim_{t\to\infty} \Delta R = \frac{b}{\Omega^2} \tag{14}$$

Since $\Omega > \Omega_s$, a radial feedback can reduce the residual radius error.

3. A block Diagram of Beam Control System

In Fig.4, a complete block diagram of beam control system is shown, where $\Delta\omega$ denotes the frequency deviation of the bucket, and $\Delta\phi_p$ represents the external phase manipulations. $\Delta\phi_d$ and ΔR_d can be used to represent the beam initial phase and radius deviation offsets and the disturbances.

Also since the beam frequency deviation $\Delta\omega_b$ and radial deviation ΔR differ only by a constant a, the typical output of the beam control system can be represented by $\Delta\phi$ and ΔR.

Note that the phase manipulation signal $\Delta\phi_p$ differs from the driving frequency error $\delta\omega$ only by a factor of k_1, therefore the fundamental system inputs can be considered as $\delta\omega$, $\Delta\phi_d$ and ΔR_d, or $\Delta\omega_d$.

Consequently, the basic system performance can be represented by the equations (10) and (11), as well as the following four equations.

$$\Delta R = T_7\,\Delta\phi_d = \frac{bs}{s^2 + k_1 s + \Omega^2}\,\Delta\phi_d \tag{15}$$

$$\Delta\phi = T_8\,\Delta\phi_d = \frac{s^2}{s^2 + k_1 s + \Omega^2}\,\Delta\phi_d \tag{16}$$

$$\Delta R = T_9\,\Delta R_d = \frac{s^2 + k_1 s}{s^2 + k_1 s + \Omega^2}\,\Delta R_d \tag{17}$$

$$\Delta\phi = T_{11}\,\Delta R_d = \frac{(a - k_1 k_2)s}{s^2 + k_1 s + \Omega^2}\,\Delta R_d \tag{18}$$

In the following studies, the phase feedback gain is represented by $G_1 = k_1$, and we also let $G_2 = k_2$. To show examples, the numerical parameters of the AGS Booster synchrotron will be introduced. At 30 ms from the beginning of the cycle, the synchrotron oscillation frequency Ω_s is about $314 \times 10^2 rad/sec$, i.e., 5 KHz. Other useful

system parameters are,

$V = 90\ KV.$

$\phi_s = 0.24\ rad = 13.7°.$

$\beta = 0.757.$

$E = 1.435 \times 10^9\ eV.$

$\omega_{id} = 3.388 \times 10^6 \times 2\pi = 2.129 \times 10^7\ rad/\text{sec}.$

$\eta = -0.385.$

$a = 6.124 \times 10^6\ rad/(m \times \text{sec}).$

$b = -161\ m/(rad \times \text{sec}).$

With phase plus radial feedback, the natural frequency is chosen as $\Omega^2 = 592 \times 10^7$. Under this condition, three different gains of k_1 will be considered and the resulting situations will be compared. These are, $k_{11} = 77 \times 10^3$, representing underdamping, $k_{12} = 154 \times 10^3$, representing critical damping, and $k_{13} = 308 \times 10^3$, representing overdamping. These parameters are chosen under the limitation posed by the delays in the beam control loops.

III. TOPICS ON RF BEAM CONTROL

In the following, we will discuss some typical situations arising in the operation of a synchrotron, using the model presented in Section II.

1. Accelerating Frequency Error

For an accelerating frequency error $\delta\omega$, the radius and phase responses are shown in Figs. 5 and 6, following equations (10) and (11), respectively. The frequency error is assumed to be 0.1 percent, i.e., $\delta\omega = 213 \times 10^2\ rad/sec$. For comparison, the responses corresponding to three different dampings are plotted.

The residual radius and phase errors can be shown as

$$\lim_{t\to\infty} \Delta R = \lim_{s\to 0} sT_5 \times \frac{1}{s} = \frac{b}{\Omega^2} \tag{19}$$

$$\lim_{t\to\infty} \Delta\phi = \lim_{s\to 0} sT_6 \times \frac{1}{s} = 0 \tag{20}$$

It is indicated in Fig.5 that the residual radial error is $\frac{213 \times 10^2 \times b}{\Omega^2} = 5.8 \times 10^{-4} m$, and in Fig.6 that the residual phase error is zero. Since k_2 is always chosen such that $bk_1k_2 >> \Omega^2$, therefore from (19) the residual radius error ratio can be approximated by $\frac{1}{k_1k_2}$.

In the design, first the required residual radius error ratio and the damping ratio have to be specified. Then by solving equations (13) and (19), together with (12), the gains k_1 and k_2 can be found.

In Fig.6 the responses clearly show two different time constants in the rising and in the falling. To estimate the time constant in the rising, we let

$$\lim_{s\to\infty} T_6 \approx \frac{1}{s + k_1} \tag{21}$$

and to estimate the time constant in the falling, we let

$$\lim_{s\to 0} T_6 \approx \frac{s}{k_1 s + \Omega^2} \tag{22}$$

where we note that $s \to \infty$ and $s \to 0$ represent the properties of the transfer function at $t \to 0$ and $t \to \infty$, respectively. Therefore the rising time constant τ_1 can be estimated to be equal to $\frac{1}{k_1}$, and the falling time constant τ_2 can be estimated by $\frac{k_1}{\Omega^2}$. It is clear that as k_1 increases, the difference between τ_1 and τ_2 will be larger, as shown in the responses in Fig.6. These informations are useful in estimating the system responses.

2. Lock-in Range and the Inner Loop

The phase lock-in range can be estimated by only considering the inner loop, which consists of the integrator (phase detector) along with the phase feedback. If only this loop is considered, the transfer function from the accelerating frequency error to the phase deviation becomes

$$\Delta\phi = \frac{1}{s + k_1}\,\delta\omega \tag{23}$$

Therefore, the lock-in range is estimated as the unity gain bandwidth of this loop, which is roughly equal to k_1, and is 154×10^3 *rad*/sec $= 24.5$ *KHz*. The higher the k_1, the larger the lock-in range. One has however to assure that the phase detector and the control circuitry is not being saturated before reaching the lock-in range.

Typically, the phase detector has a linear range of about $\pm$ 1 rad. From Fig.6, it is indicated that the maximum phase deviation due to a 0.1 percent step accelerating frequency error is 5.8 degrees with $k_{12} = 154 \times 10^3$. Therefore if only the phase detector range is considered, we estimate that the maximally allowed accelerating frequency error can be about 1 percent, i.e., 34 *KHz*. This range is larger than, but not far from, the estimated phase lock-in range. Sometimes, people use this saturation range to estimate the lock-in range.

The bandwidth of the inner loop is usually considerably wider than that of the synchrotron oscillation loop. For example, the bandwidth of the inner loop is 154×10^3 *rad*/sec with k_{12}, and the synchrotron oscillation is only 314×10^2 *rad*/sec. This is basically because of the fact that the synchrotron oscillation and the radial feedback have to go through the integration represented by $\frac{b}{s}$.

There are several issues of interest that are related to the inner loop. First let us recall the two time constants of the response discussed in the last subsection and shown in Fig.6. It is clear by inspection that the inner loop is responsible for the ris-

ing, i.e., the bandwidth of the inner loop determines the rising time constant. Secondly, for an accelerating frequency error, the larger the inner loop gain, the smaller the phase deviation. Furthermore the smaller the phase deviation, the more sluggish the radial motion. Since the system settles at a certain level of radial deviation as shown in Fig.5, then this means a longer settling time. This explains that as k_1 increases, the system becomes more overdamping. Note that the situation of underdamping is not concerned here. In the last, one cannot assume all the bunches are the same and equally spaced, then the phase detector may receive a frequency component that equals the revolution frequency. If the inner loop gain is high enough, then the phase feedback may cause unnecessary phase perturbation and therefore the filamentation. We will not however pursue further on this aspect in this article.

3. Motion of the Bunch in the Bucket

The motion of the bunch can be described in phase space as shown in Fig.7. Since one would like to avoid undesired filamentation, it is of interest to know the bunch motion with respect to the bucket. The amount of motion of the bunch with respect to bucket can be used as a criterion for the degree of the filamentation. Because the bucket itself is moving during the transient period, the plot in Fig.7 does not exactly show the motion of the bunch in the bucket. The motion of the bucket is denoted in Fig.4 by $\Delta\omega$, which is plotted in Fig.8, with a 0.1 percent accelerating frequency step error. Because of this accelerating frequency error, the bucket jumps vertically by 3.39 KHz, then the signal from the phase deviation $\Delta\phi$ is fed back to the oscillator, and the bucket is pulled back rapidly. When the phase deviation decreases, the bucket bounces back again, and finally it settles at the position that equals the final beam frequency deviation $\Delta\omega_b$. It can be concluded that the bunch phase motion in the bucket is the same as that shown in Fig.6, however the radial motion of the bunch with respect to the bucket is the difference between the bunch motion $\Delta\omega_b$ and

the bucket motion $\Delta\omega$. The motion of the bunch within the bucket can be shown in the phase space plot in Fig.9, where we note that the bucket jumps vertically by 3.39 *KHz*, hence the bunch equivalently jumps in other direction with respect to the bucket by the same amount at the onset of frequency error. The bunches are settled down finally at the center of the bucket due to the damping provided by the feedback loops.

Comparing the bunch motion in phase space shown in Fig.7 and Fig.9, one notices that the maximum frequency deviation of the bunch from the center of the bucket in Fig.9 is much larger than the bunch motion with respect to an ideal bucket as shown in Fig.7.

Let us have a detailed look at the energy deviation of the bunch with respect to the bucket. The energy deviation is related to the radial deviation as shown in Fig.1 by

$$\Delta R = \frac{-R}{\gamma_t^2 \beta^2 E} \Delta E \tag{24}$$

and the frequency deviation is related to the radial deviation by

$$\Delta\omega_b = \frac{-\omega_{id}\eta\gamma_t^2}{R} \Delta R \tag{25}$$

Thus, we get

$$\Delta\omega_b = \frac{-\omega_{id}\eta}{\beta^2 E} \Delta E \tag{26}$$

Usually, the bucket half height is defined by

$$W = \frac{\Delta E}{\omega_{id}} \tag{27}$$

In Booster, at 30 *ms* from the beginning of the cycle, $W = 0.25\ eVs$. Therefore, the bucket half height is equivalent to the energy deviation of 5.3 *MeV*. For a 0.1 percent accelerating frequency error, the bucket jumps vertically 3.39 *KHz*, which is equivalent to that the bunch jumps in an opposite direction by 2.1 *MeV*. This is

about 40 percent of the bucket half height, that implies a considerable filamentation.

Meanwhile, we recall that if only the phase lock-in range is considered, a 24.5 *KHz* accelerating frequency error can be allowed. Then, however, the bunch will jump out of the bucket. Therefore for this particular machine the lock-in range is not of concern in the design and operation. This study shows the necessity in understanding the bunch motion in the bucket.

4. Phase Manipulation

The equivalent scheme of phase manipulation control is shown in Fig.4 by $\Delta\phi_p$, which is used for changing bunch shape, debunching, transition phase shifting, and the stable phase compensation. The imbalance of the two phase shifters for the phase detector can also be simulated as a step $\Delta\phi_p$. The responses of the system in fact are the same as the accelerating frequency error responses, except that the transfer function gains differ by a factor of k_1. For step input, therefore, the responses of radial and phase deviations are the same as that in Figs. 5 and 6, though in different scalings.

For a purpose of changing bunch shape, or debunching, it is desired to move the bunch to a required position in phase space, typically at a certain phase deviation, then keep it there for a period of time. We notice that the response of the phase deviation does not follow the input signal. Thus to achieve a desired phase deviation, the control signal has to be manipulated. A typical manipulation is shown in Fig.10, where the phase manipulation signal lets the equivalent driving frequency jumping to 3.39 *KHz*, then taking a ramp, and finally turning to flat at 22.6 *KHz*. The bunch therefore can stay at a phase deviation of about 12 degrees for a period of 80 μsec. Using (4b), we know that the radial deviation is an integration of the phase deviation, then the final radial deviation can be calculated as about 0.4 *cm*.

Although the equivalent driving frequency moves away from the synchronous frequency by as much as 22.6 *KHz*, because the motion takes a relatively slow ramp, the bunch does not jump out of the bucket. The bunch motion in bucket is shown in Fig.11.

In manipulating the phase, one still observes the rule of two time constants, as shown in Fig.10 by rising and falling edges. The phase deviation flatop, however, is due to the derivative of the phase manipulation signal with respect to time. For this portion, the inner loop is again responsible. Thus, the transfer function from $\Delta\phi_p$ to $\Delta\phi$ is

$$\Delta\phi = \frac{k_1 s}{s + k_1} \Delta\phi_p \tag{28}$$

where the s in the numerator represents the derivative of the phase manipulation signal. We note

$$\frac{k_1 s}{s + k_1} = k_1 - \frac{k_1^2}{s + k_1} \tag{29}$$

After the transient response due to the second term on the right, in a time constant $\tau_1 = k_1^{-1}$, the phase deviation becomes flat, and finally it drops when the ramp of the control signal turns to flat.

5. Stable Phase Compensation

The stable phase is determined from the rate of the magnetic field variation $\dot{B}$ and the RF voltage amplitude V,

$$\phi_s = \sin^{-1} \frac{2\pi R \rho \dot{B}}{V} \tag{30}$$

where ρ is the radius of curvature of the magnets.

A stable phase variation can be considered as a disturbance at $\Delta\phi_d$. For a step $\Delta\phi_d$ of 0.1 rad, the responses of radial and phase deviations are determined by

equations (15) and (16), that are shown in Figs. 12 and 13. The response of the radius is similar to the phase deviation due to a step accelerating frequency error. The phase deviation is however different from any response that has been showed. This response again represents largely the property of the inner loop, as the time constant of settling of the response is largely determined by the inner loop bandwidth.

The bunch motion in phase space and with respect to bucket are shown in Figs. 14 and 15. Again we observe large difference in vertical motion. In Fig.15, it is shown a large vertical jump at onset. This is because that the initial phase deviation affects the bucket immediately through the phase feedback. The amount is determined by $k_1 \times \Delta\phi_d$. In this case if we take k_{12}, then the bucket jumps negatively by 2.45 *KHz*. Therefore a 0.1 *rad* step stable phase variation is significant for the filamentation.

The residual errors due to a step $\Delta\phi_d$ are as follows,

$$\lim_{t\to\infty} \Delta R = \lim_{s\to 0} sT_7 \times \frac{1}{s} = 0 \tag{31}$$

$$\lim_{t\to\infty} \Delta\phi = \lim_{s\to 0} sT_8 \times \frac{1}{s} = 0 \tag{32}$$

i.e., both are zero, which implies that if only residual errors are concerned, then the stable phase variation does not need correction.

For the transient effect, the stable phase variation can only be corrected through the phase manipulation $\Delta\phi_p$. The responses of the variation of stable phase are determined by T_7 and T_8, meanwhile the phase manipulation through $\Delta\phi_p$ induces responses as by T_5 and T_6. A perfect compensation therefore is difficult to achieve. Note that T_5 and T_6 differ T_7 and T_8, disregarding scalings, only by a differentiator s, therefore if the transient stable phase compensation is needed, a manipulation on the correcting signal from (30) by a differentiating can be considered.

With variations of $\dot{B}$ and V in the acceleration, the stable phase is also varying. It is of interest to know, for example, in determining the $\dot{B}$ and V program how

much the corresponding radius and phase deviations will be. We show in Fig.16 the radius deviation due to stable phase variation during the acceleration of the Booster, using (15). Disregarding the period of rapid variations of the stable phase during RF capture, the typical radial deviation is less than $4 \times 10^{-7}\ m$. We also calculate that the typical phase deviation is about $25 \times 10^{-9}\ rad$. Therefore, these effects are not significant. On the rapid stable phase variation, which happens at the RF capturing period, it can be calculated that the correcting signal is at a range of 0.01 percent of the accelerating frequency.

6. Injection Errors

The injection frequency error can be simulated as $\Delta\omega_d$, which is equivalent to a radius deviation of $a \times \Delta R_d$, and the injection phase error can be simulated as $\Delta\phi_d$, both in steps.

First, we discuss the frequency error. Similar to (17), the transfer function from $\Delta\omega_d$ to $\Delta\omega_b$ is

$$\Delta\omega_b = T_{11}\,\Delta\omega_d = \frac{s^2 + k_1 s}{s^2 + k_1 s + \Omega^2}\,\Delta\omega_d \tag{33}$$

The response of $\Delta\omega_b$ for 0.01 percent frequency error is shown in Fig.17. Note that the settling time is much longer than the one of $\Delta\phi$ due to $\Delta\phi_d$ as shown in Fig.13. This is because that in this case the response is dominated by the radial loop, rather than the fast inner loop.

The responses of $\Delta\omega_b$ due to a combined 0.2 rad phase error and a 0.01 percent frequency error are shown in Fig.18. It looks as if the phase error does not affect much the response. However, from the bunch motion in bucket shown in Fig.19, with only the frequency error, and the motion in bucket shown in Fig.20, with both frequency and phase errors, it is clear that the phase error causes significant bunch motion with

respect to bucket. For instance, with k_{12}, a 0.2 rad injection phase error can let the bucket to jump about 7 KHz, almost to leave the bunch out of the bucket. If the phase error cannot be reduced, then k_1 has to be reduced, or even the phase loop may have to be disconnected at the injection.

7. Magnetic Field Error

The magnetic field error has two effects. One is shown by an accelerating frequency error, due to the magnetic field error ΔB itself. This error however can be neglected provided a fast frequency synthesizer and a good magnetic field marker are available. Another is that the corresponding magnetic field variation rate $\dot{B}$ will affect the stable phase. If this variation is large, then it needs to be corrected.

We take the effect of the Booster main magnet ripple as an example. The main magnet voltage is 4.8 KV at maximum. The 1440 Hz ripple after the passive filter can be assumed to be 30 V, which corresponds to a $\dot{B} = 0.05$ $Tesla$/sec. Taking the crest RF voltage as 90 KV, following (28), the stable phase variation is calculated to be 0.09 degrees, which is negligible.

IV. Conclusion and Discussion

A simplified linear model of synchrotron oscillation under phase and radial feedback control has been introduced and several typical situations frequently appearing in accelerator operation have been studied using this model. This method provides a unified approach to the analysis of longitudinal motion in a synchrotron and the results are presented in a natural and clear fashion.

Similar method will be applied to investigate the bunch behavior during synchronous transfer between two synchrotrons, static and transient beam loadings, and the situation in passing through phase transition. Such analysis will contribute to the

design of a new synchrotron and improvement in performance of the ones under operation.

V. Acknowledgement

One of the authors (S.Y. Zhang) would like to thank E. C. Raka for several interesting discussions.

References

[1] W. T. Weng, *Fundamentals - Longitudinal Motion,* AIP Conference Proceedings, 184, pp. 243-287, 1989.

[2] U. Bigliani, *Progress Report on PSB Beam Control,* CERN SI/Int. EL/69-1, 1969.

[3] D. Boussard, *An Elementary Presentation of the PS Beam Control System,* CERN MPS/SR/Note 73-10, 1973.

[4] D. Boussard, *RF for the CERN Proton Antiproton Collider,* AIP Conference Proceedings, 153, pp. 1682-1721, 1987.

[5] K. Johnsen and C. Schmelzer, *Beam Controlled Acceleration in Synchrotrons,* CERN Symposium on High Energy Accelerators, pp.395-403, 1956.

[6] S. R. Koscielniak, *RF System Aspects of Longitudinal Beam Control,* TRIUMF Design Note, TRI-DN-91-K183, August 1991.

[7] E. Raka, *RF System Consideration for a Large Hadron Collider,* AIP Conference Proceedings, 184, pp. 288-342, 1989.

[8] W. Schnell, *Equivalent Circuit Analysis of Phase-Lock Beam Control Systems,* CERN 68-27, 1968.

[9] S. Y. Zhang and W. T. Weng, *Error Analysis of Acceleration Control Loops of a Synchrotron,* 5th ICFA Beam Dynamics Workshop, Corpus Christi, Texas, Oct. 1991.

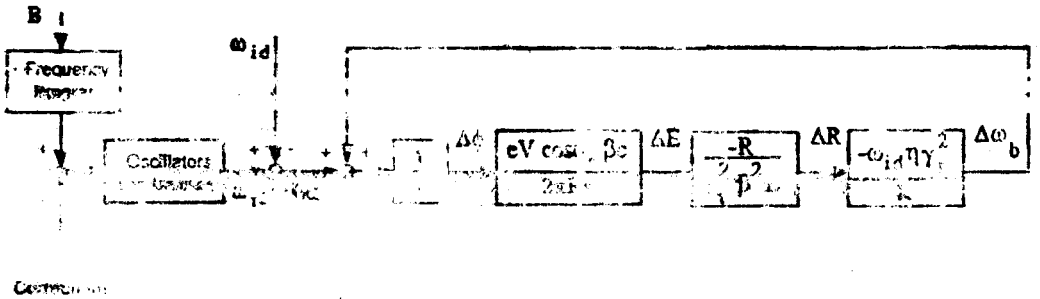

Fig. 2 Block Diagram of the Beam Dynamic Model

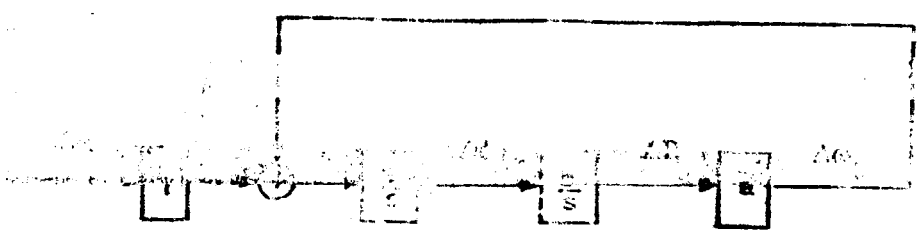

Fig. 3 Block Diagram of the Beam Dynamic Model

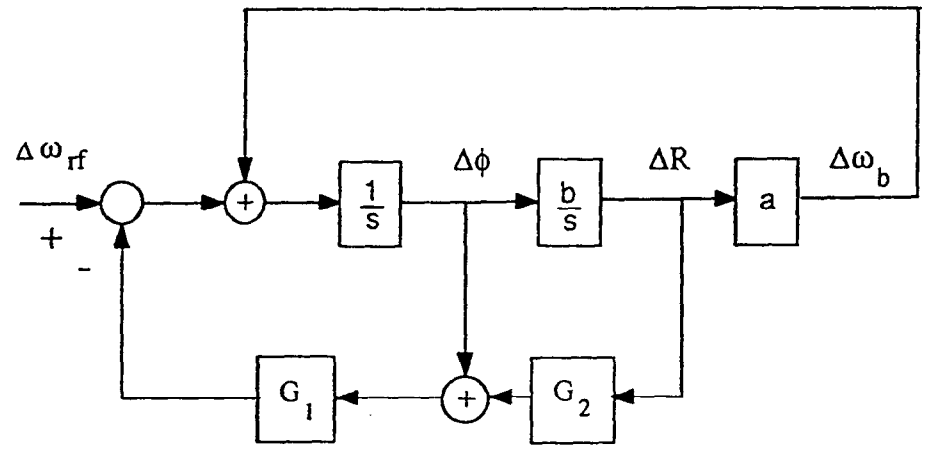

Fig.3. Block Diagram of Phase and Radial Feedbacks

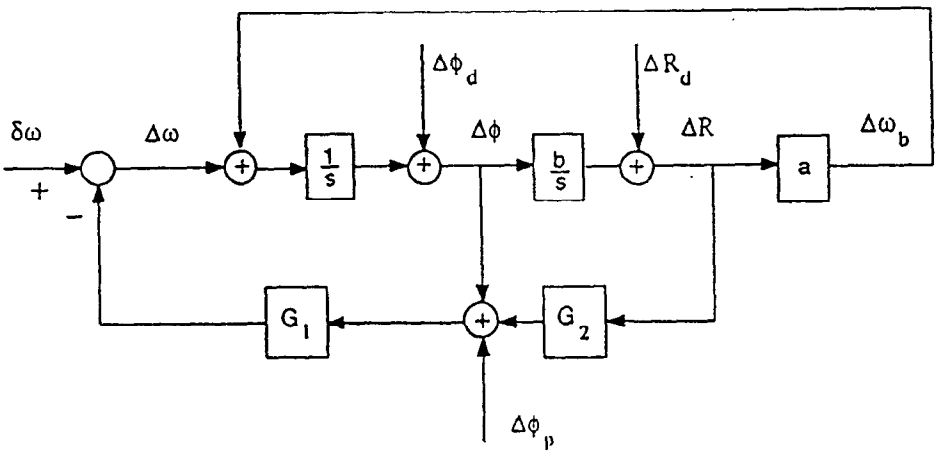

Fig.4. Block Diagram of Beam Control System

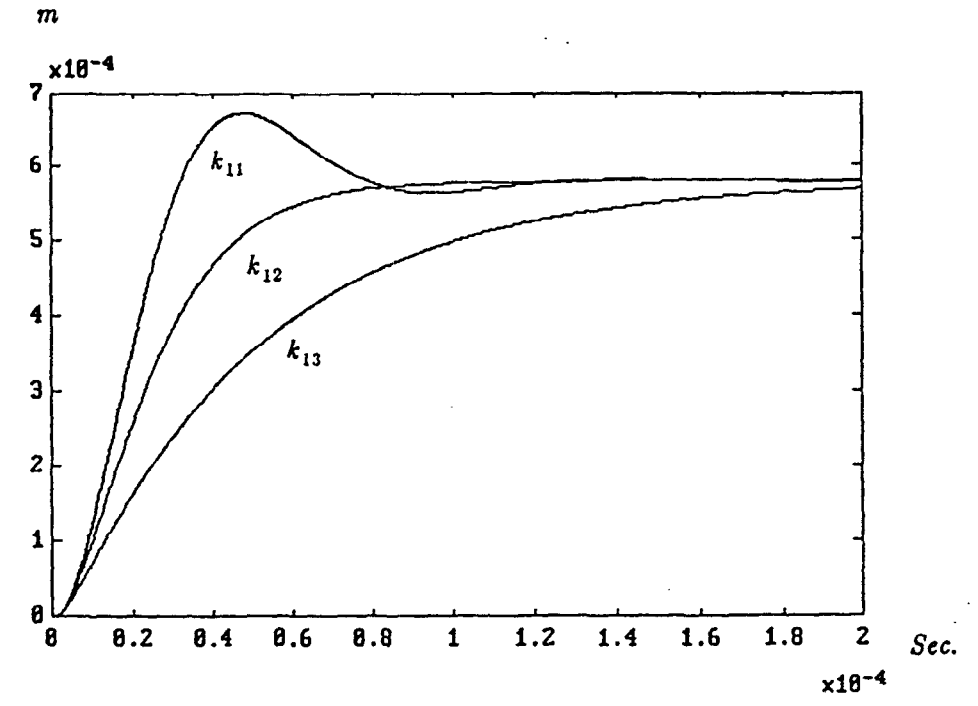

Fig.5. Radius Response due to 0.1 Percent Accelerating Frequency Error

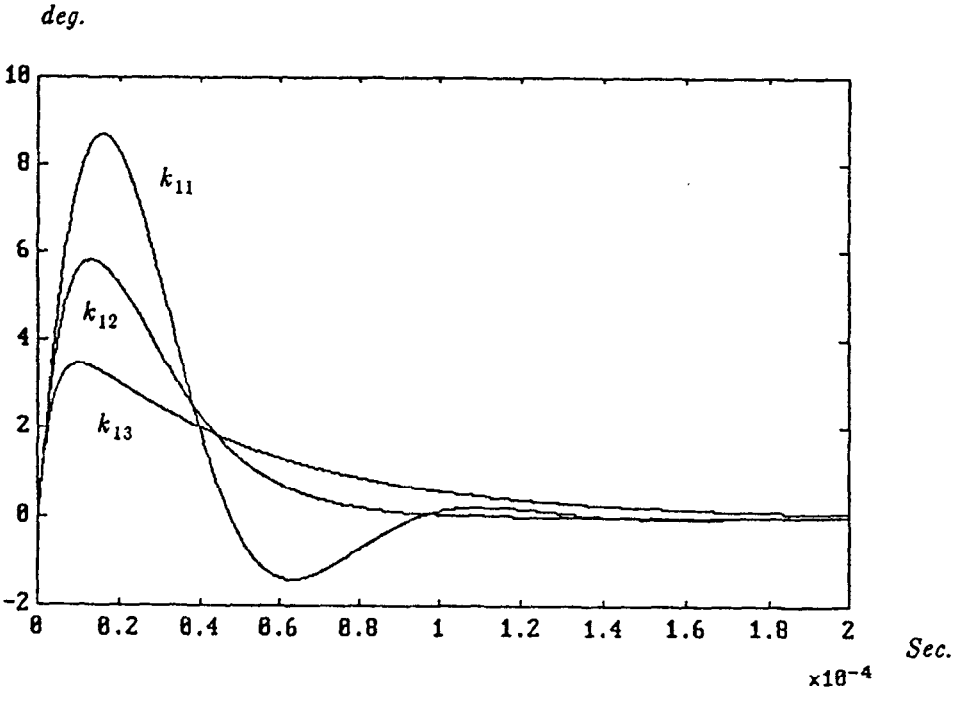

Fig.6. Phase Response due to 0.1 Percent Accelerating Frequency Error

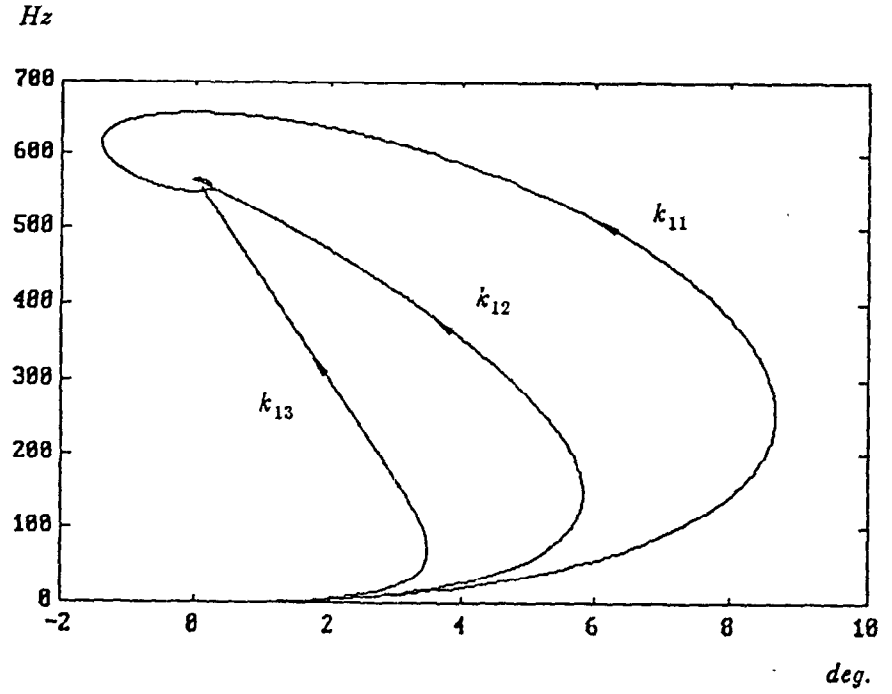

Fig.7. Bunch Motion in Phase Space. Vertical is $\Delta\omega_b$, horizontal is $\Delta\phi$.

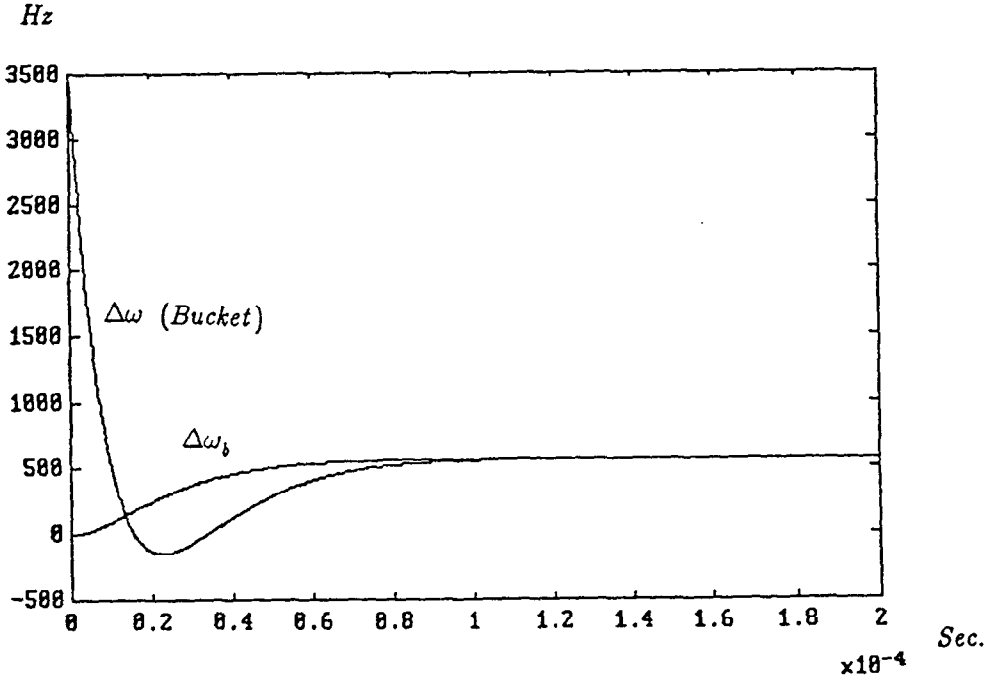

Fig.8. Motions of Bucket $\Delta\omega$ and Bunch $\Delta\omega_b$.

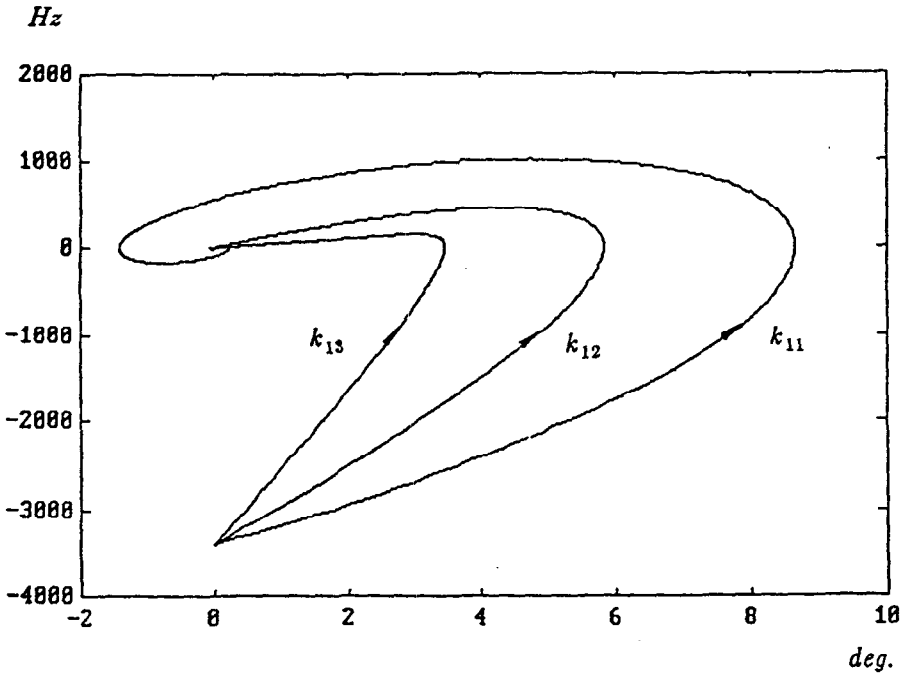

Fig.9. Bunch Motion in the Bucket. Vertical is $\Delta\omega_b - \Delta\omega$, horizontal is $\Delta\phi$.

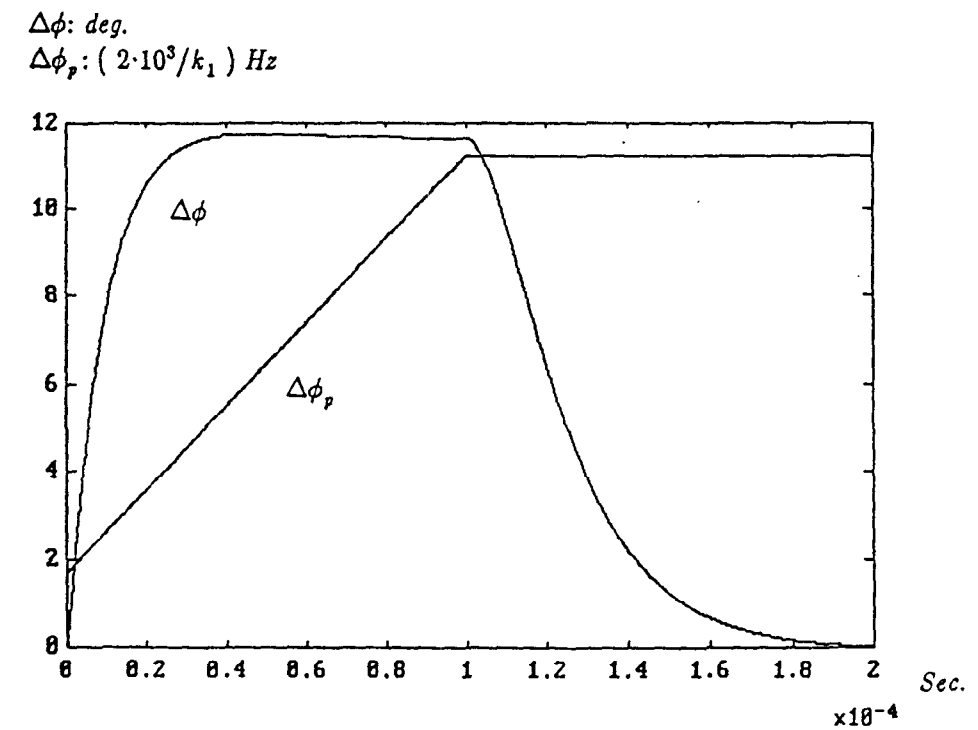

Fig.10. Phase Manipulation.

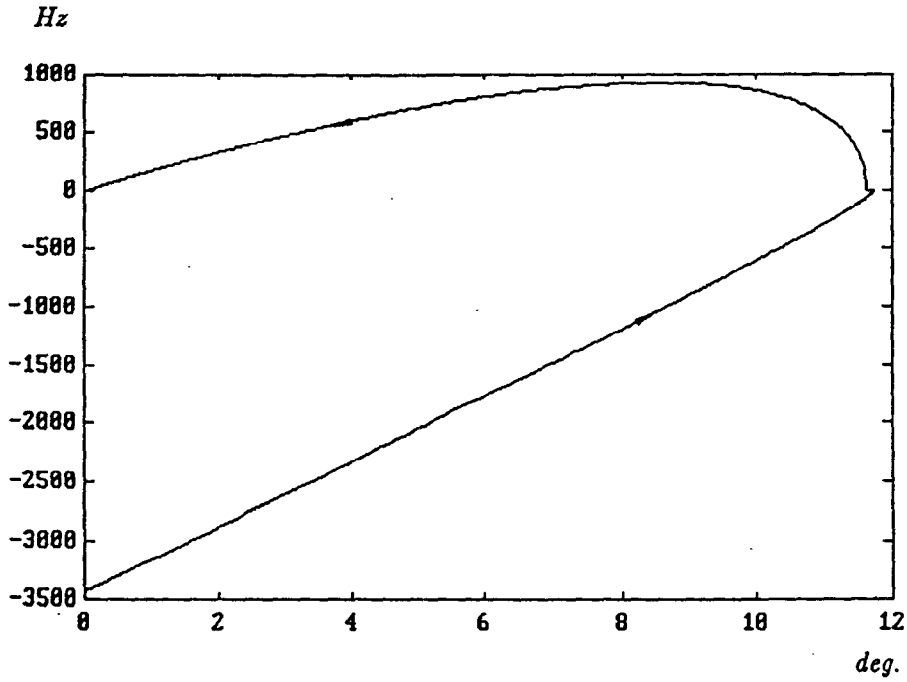

Fig.11. Bunch Motion in the Bucket for Phase Manipulation.
Vertical is $\Delta\omega_b - \Delta\omega$, horizontal is $\Delta\phi$.

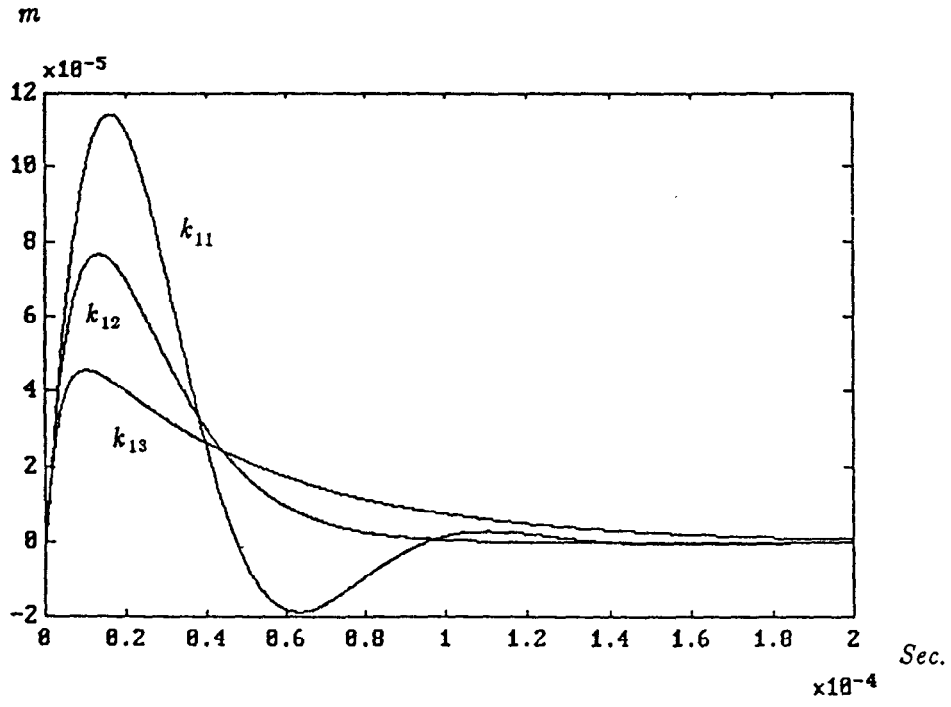

Fig.12. Radius Response due to 0.1 rad Phase Disturbance

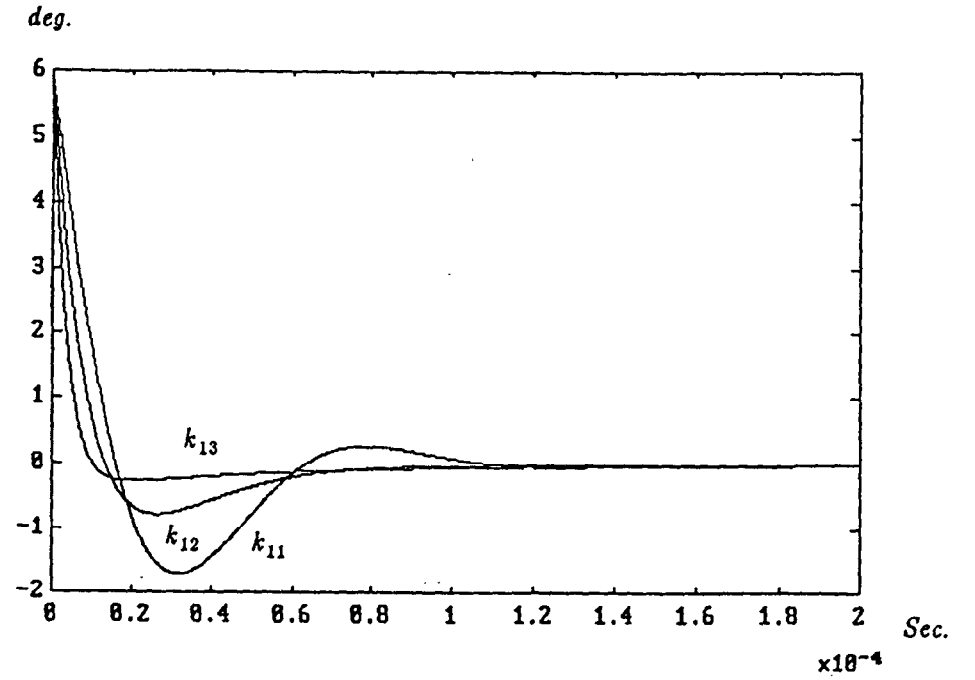

Fig.13. Phase Response due to 0.1 rad Phase Disturbance

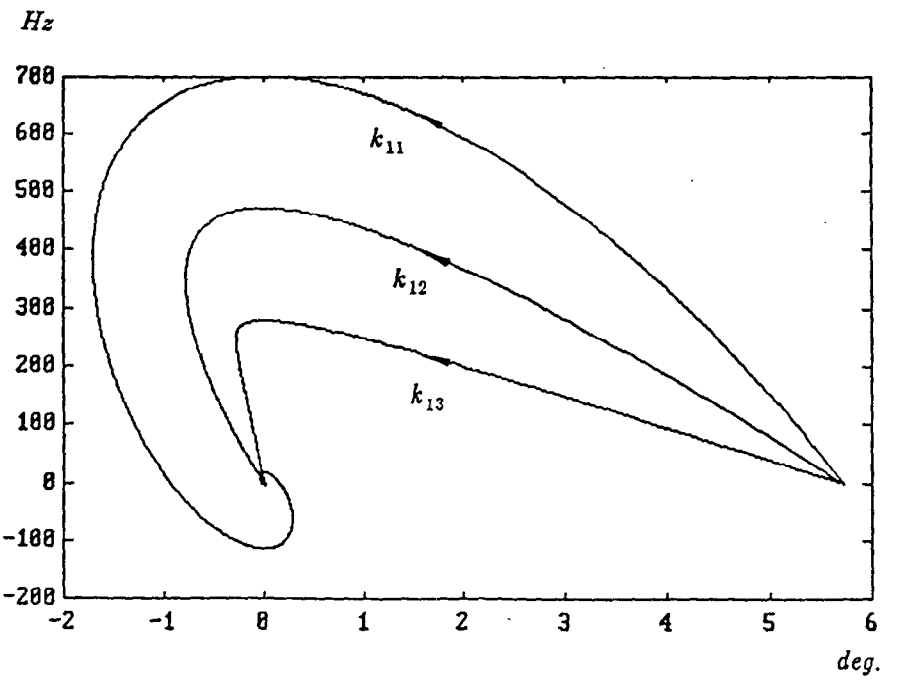

Fig.14. Bunch Motion in Phase Space for 0.1 rad Phase Disturbance.
Vertical is $\Delta\omega_b$, horizontal is $\Delta\phi$.

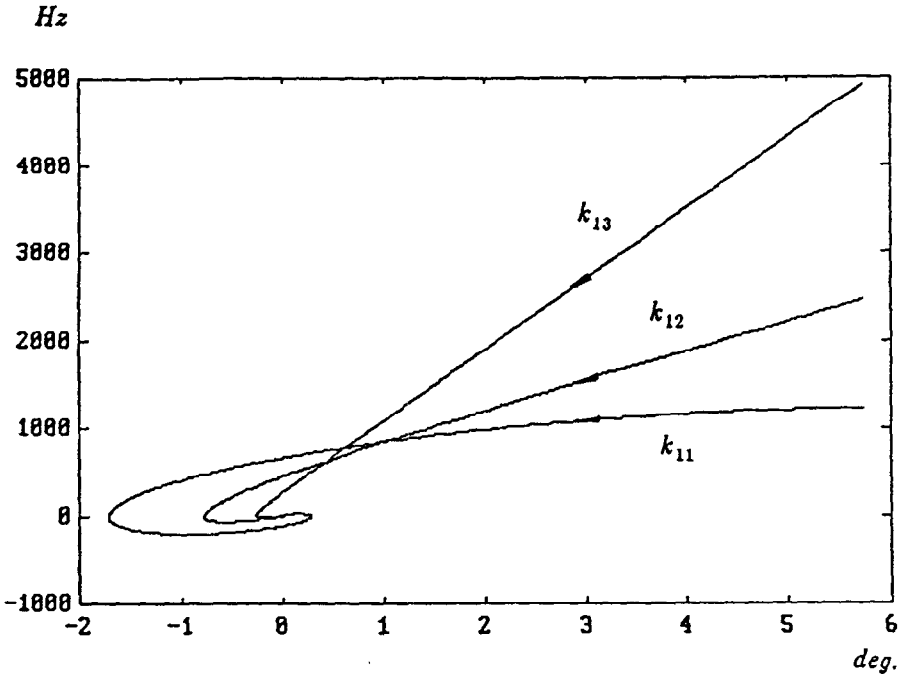

Fig.15. Bunch Motion in the Bucket, for 0.1 rad Phase Disturbance. Vertical is $\Delta\omega_b - \Delta\omega$, horizontal is $\Delta\phi$.

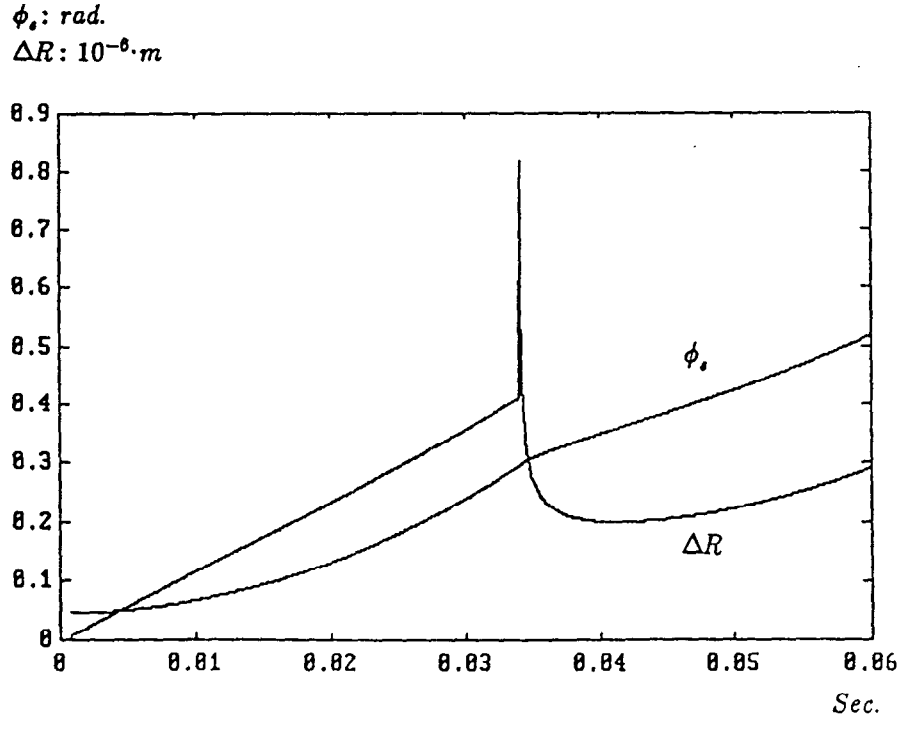

Fig.16. Radius Deviation due to Stable Phase Variation in the Booster

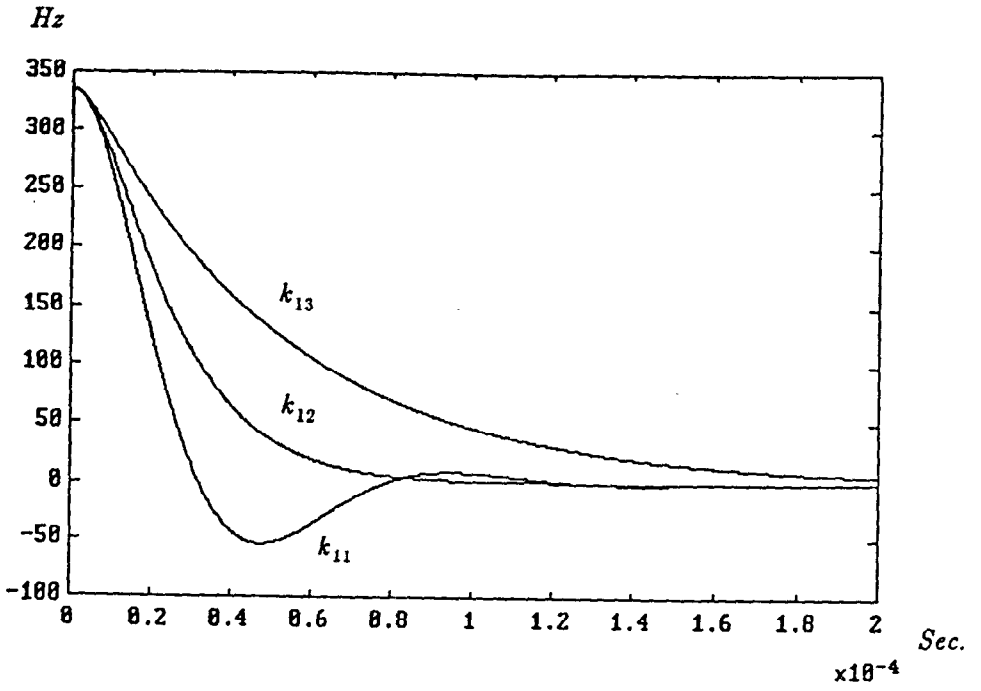

Fig.17. Frequency Response $\Delta\omega_b$ due to 0.01 Percent Injection Frequency Error

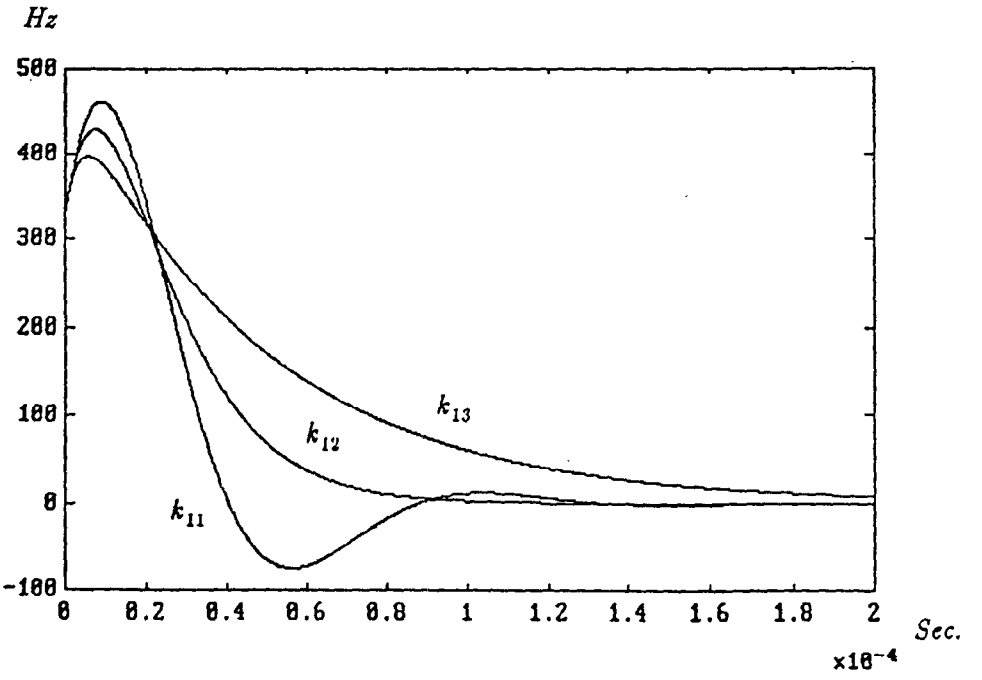

Fig.18. $\Delta\omega_b$ due to Combined 0.01 Percent Frequency Error and 0.2 rad Phase Error

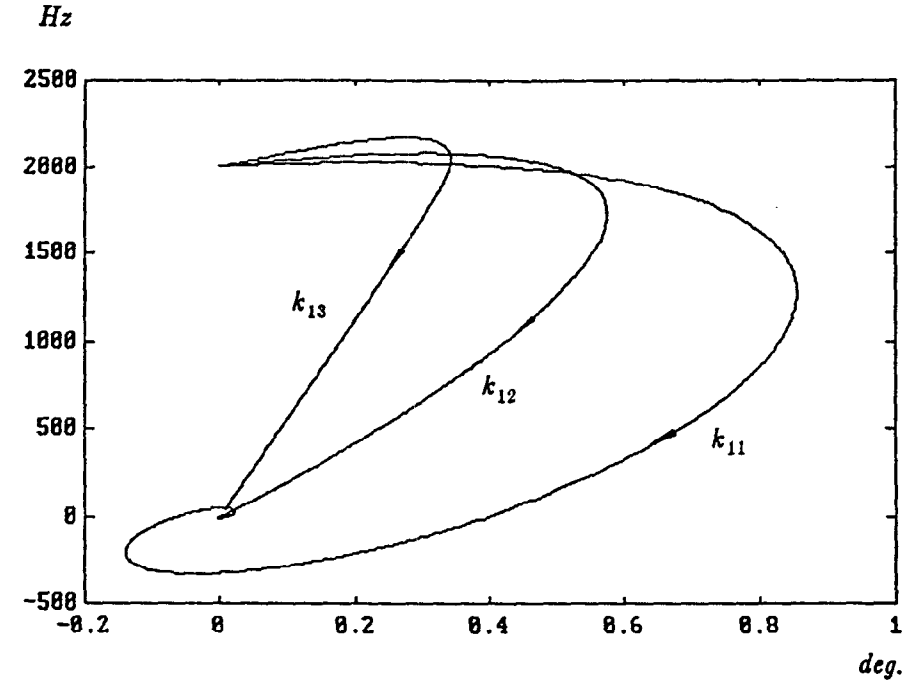

Fig.19. Bunch Motion in the Bucket, with only 0.01 Percent Frequency Error. Vertical is $\Delta\omega_b - \Delta\omega$, horizontal is $\Delta\phi$.

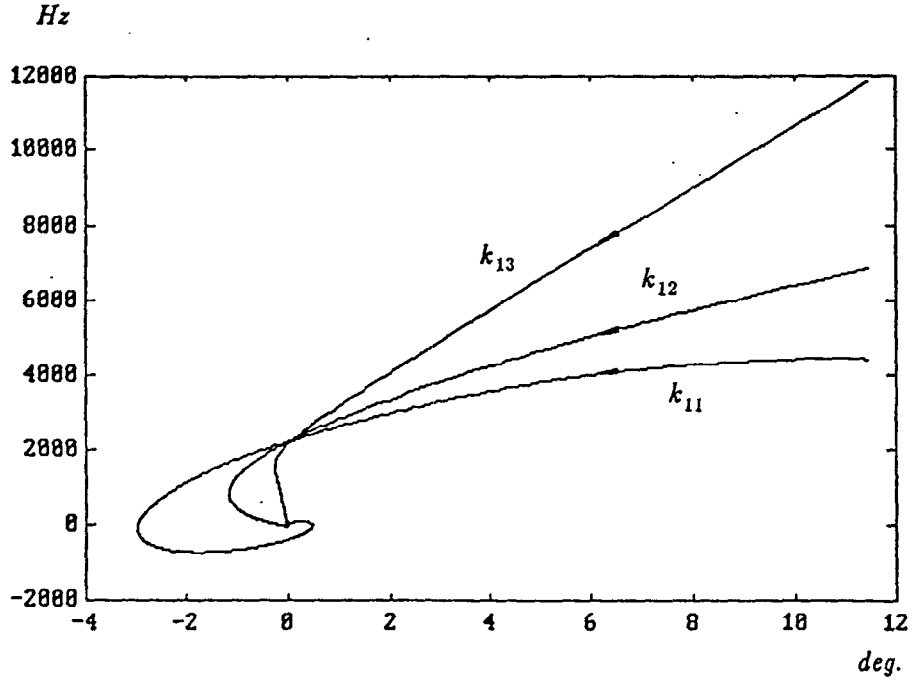

Fig.20. Bunch Motion in the Bucket with both 0.2 rad Phase Error and 0.01 Percent Frequency Error. Vertical is $\Delta\omega_b - \Delta\omega$, horizontal is $\Delta\phi$.